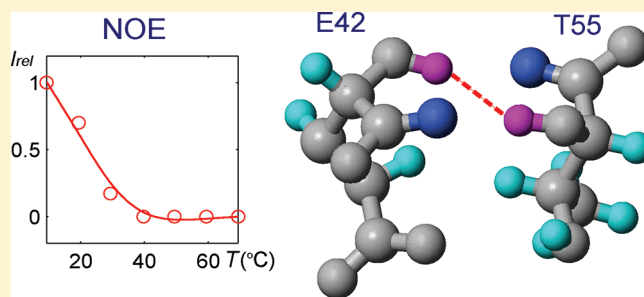


# Folding of a Tryptophan Zipper Peptide Investigated on the Basis of the Nuclear Overhauser Effect and Thermal Denaturation

Soyoun Hwang and Christian Hilty\*

Center for Biological NMR, Department of Chemistry, Texas A&amp;M University, College Station, Texas 77843, United States

**ABSTRACT:** Short, secondary-structure-containing peptides are suitable models for the study of protein folding due to their relative simplicity. Here, we investigate thermal denaturation of the tryptophan zipper peptide, trpzip4, a peptide that forms a  $\beta$ -hairpin in solution. In order to monitor the thermal denaturation of peptides or small proteins, chemical shift values of  $H^\alpha$  or  $H^N$  may be used. However, various factors other than secondary structure can influence chemical shift values, such as side-chain orientation of nearby aromatic residues. Nuclear Overhauser effect (NOE) intensity from backbone interproton cross peaks is an alternative way to study thermal denaturation, as long as various factors that give rise to a change in NOE intensity upon changing the temperature are considered. As a relative indicator for denaturation, we define a cutoff temperature, where half of the initial NOE intensity is lost for each backbone interproton cross peak. For trpzip4, this cutoff temperature is highest for residues in the central part of the structure and lowest for residues near the termini. These observations support the notion that the structure of the trpzip4 peptide is stabilized by a hydrophobic cluster formed by tryptophan residues located in the central region of the  $\beta$ -hairpin.



## INTRODUCTION

Peptides present attractive, simplified models for the study of protein folding. Short peptides, however, typically exhibit a large amount of conformational flexibility. Unlike in full-length proteins, it is by consequence common that secondary structure elements are not well-defined in peptides. The use of nonaqueous solvents is a popular way to induce secondary structure formation, albeit at the expense of being further removed from physiological conditions. Peptide sequences can also be designed to give rise to intrinsically higher structural stability by exploiting specific interactions. A set of peptides that adopt a remarkably stable  $\beta$ -hairpin secondary structure in water has been introduced by Cochran et al.<sup>1</sup> These tryptophan zipper peptides are mutants of the B1 domain of protein G. They contain several tryptophan residues that seem to confer stability through side chain–side chain interaction. Since their introduction, the stability and folding of trpzip peptides has been studied in various ways, including by circular dichroism (CD) and infrared spectroscopy.<sup>1–4</sup> Du et al. found that the key factors stabilizing  $\beta$ -hairpins are a turn-promoting sequence, which increases the folding rate, and interstand hydrophobic side chain–side chain interactions, which decrease the unfolding rate.<sup>3</sup> Wu et al. observed a strong impact of Trp–Trp interactions on the stability of the  $\beta$ -hairpin by substituting Trp with Val residues.<sup>5</sup> Takekiyo et al. also investigated the stability of the trpzip1 peptide by substituting Trp with Tyr, concluding that the mutation reduced the extent of  $\beta$ -hairpin structure and decreased the  $\beta$ -hairpin stability.<sup>6</sup> On the basis of studies by Waters et al., aromatic–aromatic interactions give rise to a more stable  $\beta$ -hairpin structure

than aliphatic–aromatic interactions.<sup>7–9</sup> In addition, trpzip peptides are often used as a model system to study the folding mechanism of  $\beta$ -hairpins by molecular dynamics (MD) simulation.<sup>4,10</sup> Gao et al. analyzed the thermodynamics involved in the folding of trpzip2, suggesting the existence of various short-lived folding intermediates that result in a zip-out folding mechanism. They also found that hydrophobic interaction between tryptophan residues of trpzip4 plays an important role in stabilizing the peptide structure.<sup>11,12</sup>

While several structures of trpzip peptides have been solved by nuclear magnetic resonance (NMR), folding and stability was predominantly investigated by other methods. NMR would present a significant opportunity to elucidate folding mechanisms because sequence positions can be individually addressed. A wealth of information on protein dynamics is, in principle, available from heteronuclear relaxation experiments. However, due to the low cost for the solid-phase synthesis of unlabeled peptides, homonuclear NMR remains a mainstay for structural study of small peptides. Peptide folding may be studied by NMR through observation of chemical shift changes, such as  $H^\alpha$  and  $H^N$ . NOEs traditionally are not often used in combination with thermal denaturation, perhaps due to the dependence of the NOE not only on the structure but also on other parameters such as the motional correlation time that changes as a function of temperature. Here, we make the case that despite these effects,

Received: July 7, 2011

Revised: October 30, 2011

Published: October 31, 2011

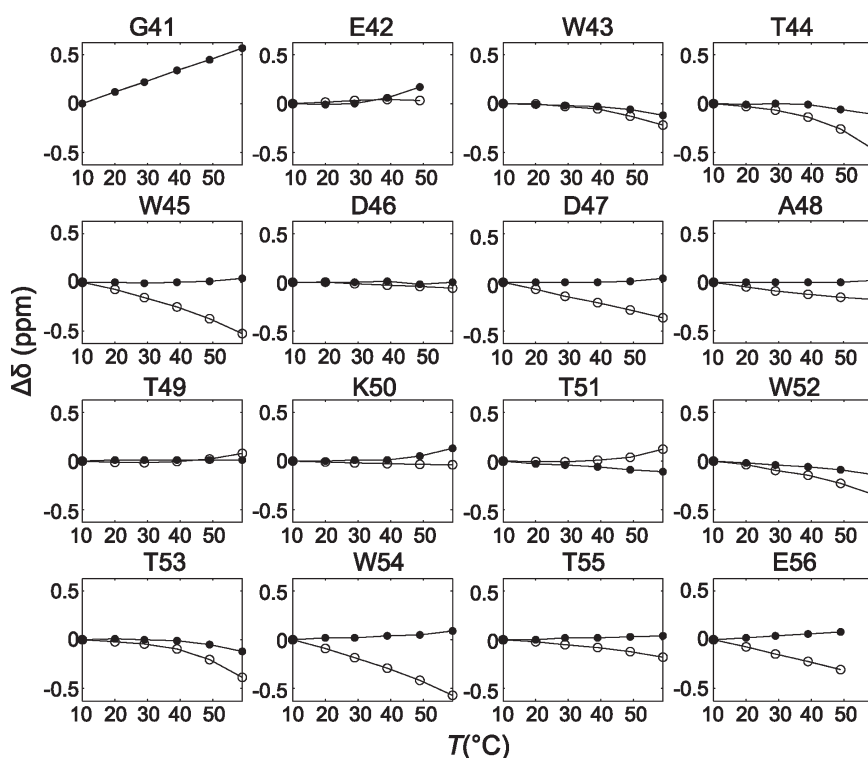


**Figure 1.** Chemical shift change of amide protons (○) and alpha protons (●) as a function of temperature (the data point at 69 °C is not plotted due to low intensity).

NOEs may still contain more information than other experimentally accessible parameters and provide a different perspective on peptide folding.

## EXPERIMENTAL SECTION

**Sample Preparation.** A peptide with the trpzip4 sequence GEWTWDDATKTTWTWTE (with sequence position numbers 41–56)<sup>1</sup> was obtained commercially from solid-phase synthesis (Anaspec, Fremont, CA) and used without further purification. The peptide was dissolved to a 1 mM final concentration in 92% water/8% deuterium oxide, containing potassium phosphate (30 mM PO<sub>4</sub>, pH 6.0) and a small amount of 4,4-dimethyl-4-silapentane-1-sulfonic acid (DSS) for chemical shift referencing. The NMR sample was sealed under argon.

**NMR Spectroscopy.** NMR spectroscopy was performed on a spectrometer with 500 MHz <sup>1</sup>H frequency equipped with a cryoprobe (Bruker, Billerica, MA). A set of NOESY (300 ms mixing time), ROESY (200 ms mixing time, with a spinlock field of 3.54 kHz), and TOCSY (100 ms mixing time) spectra was acquired for each of the following temperatures: 9, 19, 29, 40, 49, 59, and 69 °C. ROESY spectrum was acquired under unbuffered condition. 1D H/D exchange experiments were measured at 9 °C immediately after lyophilized peptide was dissolved in 100% D<sub>2</sub>O (30 mM PO<sub>4</sub>, pD 6.0).

**Data Processing.** NMR spectra were processed with the program TOPSPIN (Bruker). Peak volumes were determined using the program CARA.<sup>13</sup> Experimental data were fitted in MATLAB (Mathworks, Natick, MA). Calculated curves for the signal intensity were plotted using Mathematica (Wolfram Research, Champaign, IL). Figures with protein structures were prepared using PyMOL (open source version, Schrödinger LLC, Portland, OR).

## RESULTS AND DISCUSSION

In order to assess thermal denaturation of trpzip4, NMR measurements were carried out over an accessible temperature range between 9 and 69 °C (see Experimental Section). Loss of the folded structure of the peptide in this temperature range can also be assessed by CD spectroscopy. According to CD measurements (from ref 1 and in agreement with data collected of the samples used here, not shown), the peptide has approximately reached the midpoint of thermal denaturation at 69 °C, the highest temperature used. Because the CD spectrum of trpzip4 is dominated by exciton coupling between the aromatic chromophores of tryptophan, the parameter that is accessible in these measurements is not directly the amount of secondary structure but rather the mutual proximity of tryptophan side-chain moieties.

**NMR Chemical Shifts.** Generally, the chemical shift of amide protons in the polypeptide is expected to decrease as the temperature increases, that is, the amide proton becomes more shielded.<sup>14–19</sup> In trpzip4, the majority of amino acids follow this pattern (Figure 1). However, Thr 49 and Thr 51 show opposite behavior. It can also be seen that the chemical shifts of the amide protons of Trp 45 and Trp 54 are most temperature-dependent, such that it may be hypothesized that a change in local structure, such as the side-chain orientation of tryptophan residues, may have a dominating effect on the chemical shift.<sup>17,18</sup> On this premise, the chemical shift, while indicating structural changes in the peptide, may not be a faithful measure specifically for the loss of the hydrogen bonds that define  $\beta$ -sheet secondary structure. Furthermore, previous studies have found that amide proton temperature coefficients do not correlate well to hydrogen bonding in peptides.<sup>17,20</sup>

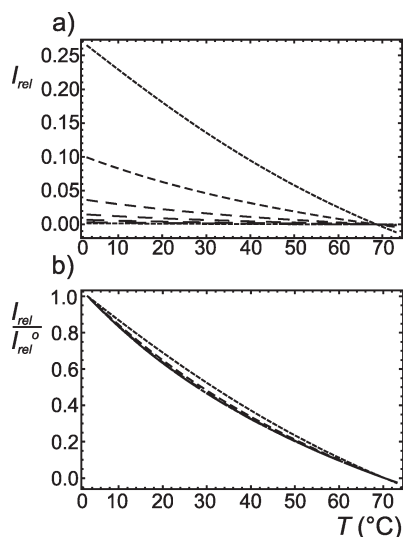


**Figure 2.** (a) NOE cross peak intensity calculated for an isolated pair of protons in a rigid molecule, as a function of temperature. (b) Intensity curves scaled to unit intensity at 0 °C (273 K). Dashed lines indicate interproton distances from 0.2 to 0.5 nm, in steps of 0.05 nm, from the shortest to longest dash. Curves were calculated for a particle with a radius of gyration of 1.0 nm, a field strength of 11.74 T, and a NOE mixing time of  $t_{\text{mix}} = 0.3$  s. The abscissa is shown in units of °C for readability.

Apart from amide protons, the alpha proton chemical shift values can be used to estimate the secondary structure of a protein.<sup>21</sup> In Figure 1, changes in the chemical shift of  $\text{H}^\alpha$  protons are relatively small, possibly because the highest temperature accessible in the NMR experiments reaches only the midpoint of denaturation, as indicated by CD spectroscopy.

**Nuclear Overhauser Effect.** Because the nuclear Overhauser effect is highly sensitive to changes in interproton distance, it would appear to be a natural choice for assaying denaturation. Moreover, while the  $^1\text{H}$ – $^1\text{H}$  NOE is not observed directly at the location of the interstrand hydrogen bond, distances  $d\text{H}^\alpha\text{H}^\alpha(i,j)$ ,  $d\text{H}^\text{N}\text{H}^\text{N}(i,j)$ , and  $d\text{H}^\alpha\text{H}^\text{N}(i,j)$  observed by NOE are deemed characteristic for the presence of an antiparallel  $\beta$ -sheet structure, and distances  $d\text{H}^\text{N}\text{H}^\text{N}(i,j)$  and  $d\text{H}^\alpha\text{H}^\text{N}(i,j)$  are for a parallel  $\beta$ -sheet structure.<sup>22</sup> When attempting to use the NOE for assaying thermal denaturation, it is necessary to consider various factors that can give rise to a change in NOE intensity upon changing the temperature. For an isolated pair of protons, the cross peak intensity in a transient NOE experiment is given as

$$I_{\text{NOE}} = \sinh(-\sigma t_{\text{mix}}) \exp(-\rho t_{\text{mix}}) \quad (1)$$

where  $t_{\text{mix}}$  is the NOE mixing time and the autorelaxation rate  $\rho$  and cross-relaxation rate  $\sigma$  are given as

$$\rho = \frac{\gamma^4 \hbar^2 \mu_0^2}{64\pi^2 r^6} (J(0) + 3J(\omega) + 6J(2\omega)) \quad (2)$$

$$\sigma = \frac{\gamma^4 \hbar^2 \mu_0^2}{64\pi^2 r^6} (-J(0) + 6J(2\omega)) \quad (3)$$

Here,  $r$  is the distance between the two protons,  $\omega$  is the angular frequency of spin precession,  $\gamma$  is the gyromagnetic ratio,  $\hbar$  is the reduced Planck constant, and  $\mu_0$  is the vacuum permeability.<sup>23</sup> In spin relaxation experiments, the spectral density is often approximated

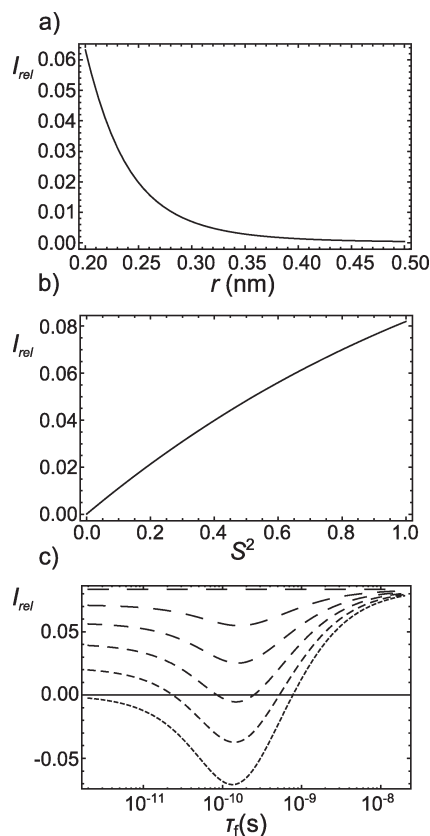


**Figure 3.** Curves illustrating the dependence of the NOE cross peak intensity for an isolated proton pair on (a) the interproton distance  $r$ , (b) the Lipari–Szabo order parameter  $S^2$ , and (c) the correlation time  $\tau_f$  for fast internal motion. The common parameters are identical to those in Figure 2. Curves were plotted for a constant temperature of  $T = 40$  °C (313 K), resulting in  $\tau_c = 1$  ns. Parameters specific to the individual panels are as follows: (a)  $S^2 = 0.7$ ; (b)  $\tau_f = 0$  (fast intramolecular motion limit),  $r = 0.2$  nm; and (c)  $S^2$  varying from 0 to 1 in steps of 0.2 for curves from the shortest to longest dash in the bundle,  $r = 0.2$  nm.

by the model-free expression of Lipari and Szabo.<sup>24,25</sup>

$$J(\omega) = \frac{2}{5} \left( S^2 \frac{\tau_c}{1 + \omega^2 \tau_c^2} + (1 - S^2) \frac{\tau_f'}{1 + \omega^2 \tau_f'^2} \right) \quad (4)$$

$\tau_c$  is the correlation time for global motion,  $S^2$  is an order parameter for the accessible local conformations, and  $\tau_f' = \tau_f/(\tau_f/\tau_c + 1)$ , with  $\tau_f$  as a correlation time for fast internal motions. In the case of a rigid molecule ( $S^2 = 1$ ), this spectral density reduces to the usual expression and depends only on the global correlation time. The temperature dependence of  $\tau_c$  can be approximated as

$$\tau_c = \frac{4\pi\eta a^3}{3kT} \quad (5)$$

with  $a$  as the radius of gyration of the polypeptide,  $k$  as Boltzmann's constant, and  $T$  as the temperature.<sup>22</sup> Over the temperature range used, the most significant effect of the temperature on  $\tau_c$  lies in the change in the dynamic viscosity of the solvent, which for water is approximated by  $\eta = (0.4508 \text{ N s m}^{-2}) e^{-(0.02076 \text{ K}^{-1})T}$ , based on data encompassing the temperature range between 9 and 69 °C.<sup>26</sup> The effect of the temperature dependence of  $\tau_c$  on the observed NOE cross peak

**Table 1.** Amide Proton Exchange Rates Per Residue of trpzp4<sup>a</sup>

residue	rate constant (h <sup>-1</sup> )	residue	rate constant (h <sup>-1</sup> )
W43	>10	T51	0.3
T44	0.4	W52	6.2
W45	>10	T53	0.4
D46	0.2	W54	>10
D47	>10	T55	2
A48	8	E56	4
K50	0.3		

<sup>a</sup> Rates for E42 and T49 were not determined due to spectral overlap with tryptophan signals.

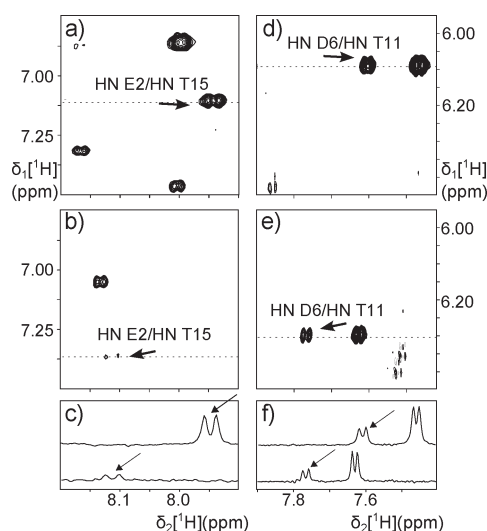


**Figure 4.** Extracts from 2D-<sup>1</sup>H,<sup>1</sup>H NOESY spectra of trpzp4, showing the cross peaks E42-T55 and D46-T51. The spectra were measured (a,d) at 9 °C and (b,e) at 29 °C. (c) E42-T55 and (f) D46-T51 show one-dimensional slices through the cross peaks, taken from the positions indicated by the dotted lines in (a, b, d, and e).

intensity is examined in Figure 2 under the assumption of a pair of protons in a rigid molecule using parameters similar to those expected for a peptide the size of trpzp4. The absolute NOE intensity is strongly distance-dependent (see Figure 2a). However, its relative reduction as a function of increasing temperature is nearly equal for the typically observed distances between 0.2 and 0.5 nm (Figure 2b). This observation forms the basis for considering the NOE cross peak intensity as an indicator for protein denaturation. Any differences in the intensity as a function of temperature among the various observed cross peaks would be expected to arise from changes in the peptide itself, as opposed to merely from differences in initial proton–proton distance.

NOE cross peak intensities are influenced by both structural and dynamic factors, which need to be considered. The strong dependence on internuclear distance (Figure 3a) is well-known. It may further be noted that this plot assumes an isolated pair of protons, such that both auto- and cross-relaxation rates decrease with increasing distance. In the real situation, where third protons give additional contributions to relaxation, the decrease in cross peak intensity with increasing distance may be even stronger. As described above, intramolecular motions of the polypeptide can

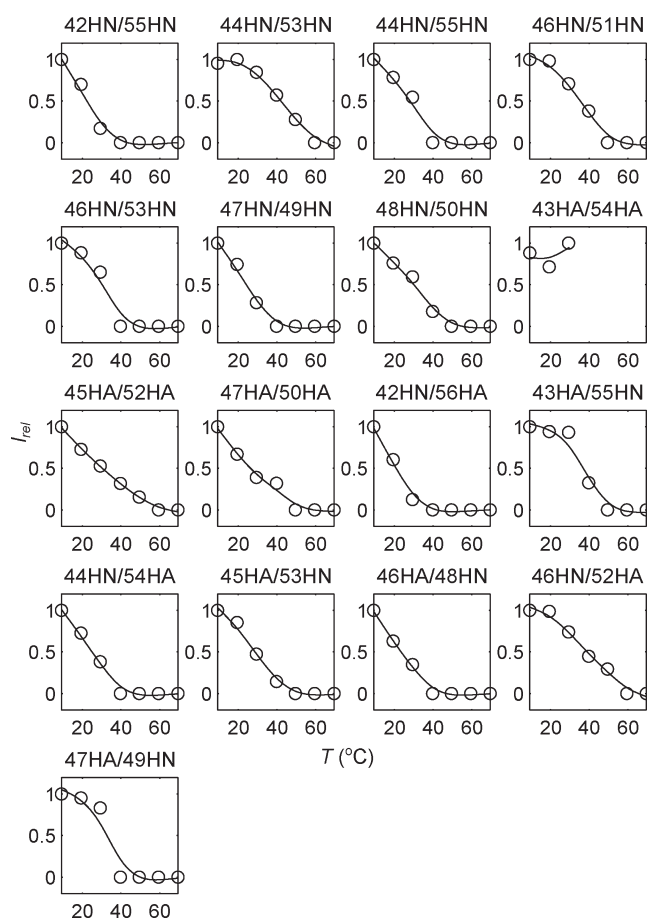


**Figure 5.** Relative intensity of backbone–backbone NOE cross peaks as a function of temperature. The line represents a cubic smoothing spline interpolation of the experimental data (see text).

be described by the two parameters  $S^2$  and  $\tau_f$ . Figure 3b shows that the cross peak intensity also decreases with decreasing order parameter, which arises due to increased sampling of conformational space. In the limit of fast intramolecular motion, as shown in the figure, the NOE vanishes for  $S^2 = 0$ . In other cases, a residual positive or negative intensity would remain. Order parameters are frequently reported in the literature for amide bonds because those can be determined from heteronuclear [<sup>1</sup>H,<sup>15</sup>N]-NOE measurements using <sup>15</sup>N-labeled proteins.<sup>27</sup> Common order parameters range from ~0.5 to 1.0 in folded proteins,<sup>27,28</sup> whereas for unfolded polypeptides, values such as from 0.2 to 0.5 have been reported.<sup>29,30</sup> Even though the polypeptide backbone proton–proton distances measured in a homonuclear [<sup>1</sup>H,<sup>1</sup>H]-NOESY experiment are different from amide bonds, it may be reasonable to expect at least similar degrees of disorder.

Upon loss of secondary structure, distances characteristic for the type of secondary structure will increase, ultimately beyond the limit detectable by NOE, while at the same time, the order parameter decreases. Both of these effects give rise to reduced NOE cross peak intensity. The third parameter,  $\tau_f$ , gives rise to a more complicated behavior. Figure 3c has been plotted with sufficient range to show the limiting cases of fast intramolecular motion, where the spectral density decreases linearly with  $S^2$ , and of slow intramolecular motion, where the spectral density reduces to that of the rigid molecule. In between lies a minimum, so that the



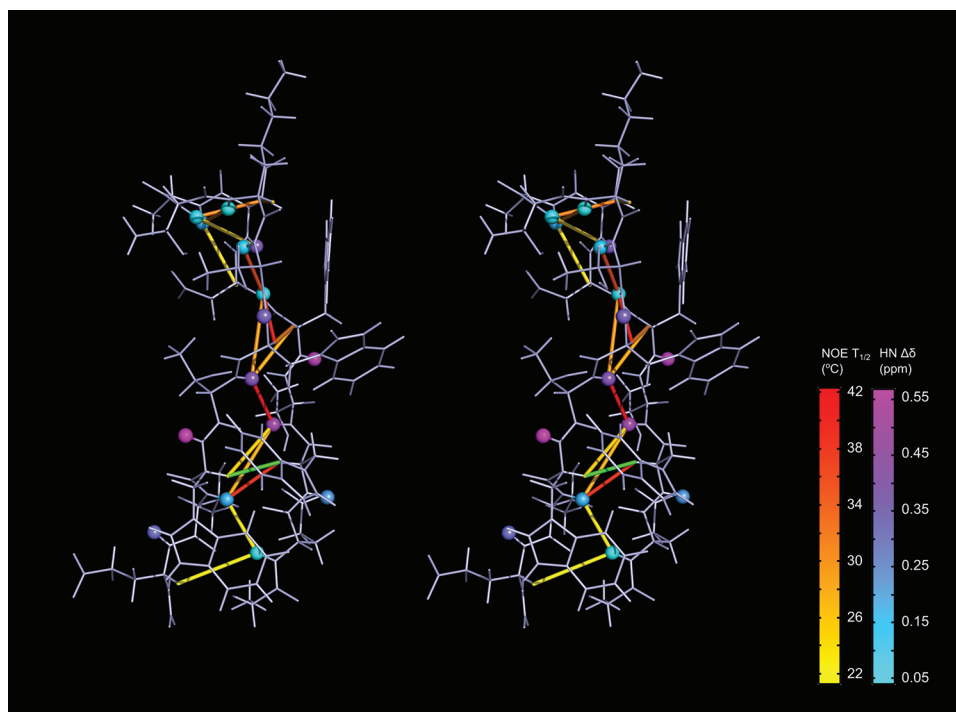


**Figure 6.** Wall-eyed stereoview of trpzip4 with backbone–backbone distances color-coded according to the temperature at which the corresponding NOE cross peak had lost half of its volume as compared to the cross peak at 9 °C. Yellow colored lines indicate cross peaks that are lost at the lowest temperature, and red colored lines those lost at the highest temperature. The green colored line is for the distance 43HA/54HA, for which the cutoff temperature could not be determined due to overlap with the water resonance (compare to Figure 5). Amide and alpha protons are color-coded according to their change in chemical shift between 9 and 69 °C. Cyan indicates a nearly constant chemical shift, and magenta indicates the largest change.

cross peak intensity in fact can increase again if  $\tau_f$  decreases below a threshold of a few hundred picoseconds. This effect is opposite to those previously discussed but, under the present conditions, appears relatively small in comparison.

In addition to the parameters considered above, effects such as the exchange of labile protons may play a further role in changing NOE cross peak intensity. While the magnitude of this effect may be more difficult to predict theoretically, it results in a loss of NOE intensity upon increased exchange due to increased temperature. It thus compounds the effect of other parameters, such as an increase in the distance upon denaturation, discussed above. Because of the various contributions, the observed NOE intensity does not directly follow the denaturation curve for the polypeptide. Nevertheless, the combination of effects that relate to denaturation is expected to give rise to loss in the NOE intensity. Therefore, the NOE has the potential to serve as an indicator for peptide denaturation.

For the trpzip4 peptide, NOEs and amide proton exchange rates can be used to confirm the secondary structure present in the peptide at the lowest temperature (9 °C). Cross peaks between  $H^N$  of Glu 42 and  $H^N$  of Thr 55,  $H^N$  of Thr 44 and  $H^N$  of Thr 53,  $H^N$  of Asp 46 and  $H^N$  of Thr 51,  $H^\alpha$  of Trp 43 and  $H^\alpha$  of Trp 54,  $H^\alpha$  of Trp 45 and  $H^\alpha$  of Trp 52,  $H^N$  of Glu 42 and  $H^\alpha$  of Glu 56,  $H^\alpha$  of Trp 43 and  $H^N$  of Thr 55,  $H^N$  of Thr 44 and  $H^\alpha$  of Thr 53, and  $H^N$  of Asp 46 and  $H^\alpha$  of Trp 52 are indicative of the antiparallel  $\beta$ -sheet secondary structure. Additionally, the presence of hydrogen bonds is confirmed by reduced hydrogen exchange rates.<sup>31</sup> Table 1 shows that amide protons of Thr 44, Asp 46, Thr 51, and Thr 53 involved in hydrogen bonds in the core of the protein have low hydrogen exchange rate constants, while solvent-exposed amide protons of Trp 43, Trp 45, Asp 47,

Ala 48, Trp 52, Trp 54, and Glu 56 have high rate constants. These data obtained from NOE and hydrogen exchange measurements agree well with the published structure, from which hydrogen bonds between  $H^N$  of Glu 42 and O of Thr 55,  $H^N$  of Thr 44 and O of Thr 53,  $H^N$  of Asp 46 and O of Thr 51, and  $H^N$  of Thr 49 and O of Asp 46 can be predicted.<sup>1</sup>

In 2D- $[^1H, ^1H]$  NOESY spectra obtained from trpzip4 at increasing temperatures, it is readily apparent that cross peaks between different protons exhibit different temperature dependence. For example, as shown in Figure 4, the cross peak between Asp 46 and Thr 51 at 29 °C retains 70% of its intensity at 9 °C, whereas the cross peak between Glu 42 and Thr 55 retains 17% of its intensity at 9 °C. While Glu 42 and Thr 55 are located at the termini, Asp 46 and Thr 51 are located near the cross-strand interaction between Trp residues.

The temperature dependence of all of the observed cross-strand NOEs that have been observed in trpzip4 is plotted in Figure 5. Most strikingly, it can be seen that these curves follow a sigmoidal temperature dependence, which stands in contrast to the convex function from Figure 2. The conclusion is that, in addition to the increased molecular motion, other changes in the polypeptide significantly contribute to the temperature dependence of NOE cross peak intensity. This experimental observation therefore lends further support to the use of the NOE for the assay of protein denaturation. At the same time, it is apparent that eqs 1–5 contain more unknown parameters than could reasonably be included in a fit, even in the absence of the effects arising from structural changes in the polypeptide. Nevertheless, in order to extract a quantitative measure reflecting the observed differences, the data of Figure 5 has been fit by cubic smoothing splines. From these splines, a fully empirical cutoff temperature,

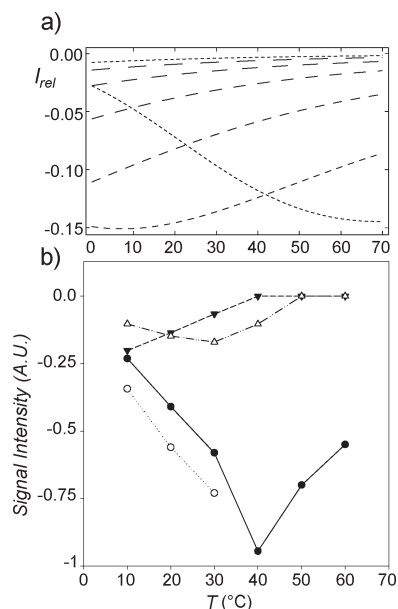


**Figure 7.** (a) Temperature dependence of the ROE effect calculated for a rigid molecule. Parameters are identical to those in Figure 2, except for the mixing time, which was 200 ms. (b) Observed ROE cross peak intensities for trpzip4 (●: 45HA/52HA; ○: 43HA/54HA; ▼: 42HN/55HN, △: 46HN/51HA).

which is defined as the temperature at which the NOE intensity falls below one-half of that at the lowest temperature measured (here, the lowest measured temperature is 9 °C) can readily be determined for each residue. Ideally, where the sigmoidal shape is fully observable in the measured temperature range, such as for the NOE between H<sup>N</sup> of Asp 46 and H<sup>α</sup> of Trp 52, this cutoff temperature should be relatively insensitive with respect to the choice of the lower-temperature limit. In other cases, where the plateau is not yet reached at the lowest temperature (e.g., 42HN/56HA), the calculated cutoff temperature may be an overestimate. Nevertheless, the thus-calculated temperature for 42HN/56HA is still lower than, for example, that for 46HN/52HA.

The distribution of cutoff temperatures is most clearly seen in Figure 6, where the corresponding distances are color-coded on the structure of trpzip4. The structure shown is used as obtained from the protein database (PDB ID 1LE3).<sup>1</sup> Interestingly, the largest cutoff temperatures are clustered in the central region of the hairpin, close to the four tryptophan residues. On the other hand, both of the regions containing the termini as well as the loop appear to show lower thermal stability. It appears likely that indeed the tryptophan–tryptophan side-chain interactions significantly contribute to the stability of the  $\beta$ -hairpin structure. This result is in good agreement with a previous study that implicated the tryptophan residues in the stability of the related peptide trpzip2, by selective mutagenesis of those residues.<sup>5</sup> A recent MD simulation study performed by Gao et al. further has predicted a disfavored turn structure for trpzip4, and a hydrophobic core centric mechanism was proposed for hairpin folding, where a strong hydrophobic interaction between tryptophan residues strengthens the stability of hydrogen bonds in the middle of the strands.<sup>12</sup>

From Figure 6, it is further apparent that a high NOE derived cutoff temperature in fact correlates to some extent with a large change in the amide proton chemical shift upon an increase of

temperature. For example, the amide protons of Thr 44 and Thr 53, which are located in the core of the hairpin, at the lowest temperature appear at a higher chemical shift than all other amide protons. They shift in the direction toward the average chemical shift with increasing temperature. Such effects are expected due to the loss of initial structure or hydrogen bonds in the core of the peptide.<sup>17</sup>

For the structural study of peptides of intermediate size, rotating frame Overhauser spectra (ROESY) are often preferred over NOESY spectra because ROESY cross peaks can be observed at all temperatures. Therefore, we have further evaluated the utility of this type of spectroscopy toward the study of the thermal denaturation process in trpzip4. From a simulation of expected ROE intensities (Figure 7a), it is apparent that, depending on the parameters, foremost the distance between atoms, the ROE is in some cases expected to initially increase with increasing temperature. This behavior was observed experimentally for the contacts between H<sup>α</sup> of Trp 43 and H<sup>α</sup> of Trp 54 and between H<sup>α</sup> of Trp 45 and H<sup>α</sup> of Trp 52 (Figure 7b). In this case, a simple empirical cutoff temperature as was used above for the analysis of NOESY spectra cannot easily be defined, and it would be necessary to employ a model that includes additional assumptions and unknown parameters. The ROE effect appears therefore less well suited for the analysis of thermal denaturation of short peptides.

## CONCLUSIONS

In summary, we have studied the thermal denaturation of the  $\beta$ -hairpin peptide trpzip4 by a NOE-based method. The results indicate that the region of highest thermal stability lies in the core region, in the vicinity of the tryptophan residues. It appears likely, therefore, that side chain–side chain interactions of these amino acids play a significant role in stabilizing the structure of trpzip4 while still preserving the native hydrogen bonds typical for an antiparallel  $\beta$ -sheet secondary structure. Methodologically, a NOE-based study appears particularly favorable compared to the more traditional chemical-shift-based measurements in cases such as here, where a change in aromatic side-chain conformation has a strong potential to influence chemical shift or where the change in chemical shift is reduced due to incomplete denaturation in the accessible temperature range. The primary limitation of the NOE-based method lies in the accessible temperature because at high temperature, the NOE intensity is reduced due to increased molecular tumbling. However, at lower temperature, corresponding to the onset of the denaturation process of peptides, it may well be more sensitive than other experimentally observable parameters.

## AUTHOR INFORMATION

### Corresponding Author

\*E-mail: chilty@chem.tamu.edu. Telephone: (979) 862-3099. Fax: (979) 862-4237.

## ACKNOWLEDGMENT

C.H. thanks the Camille and Henry Dreyfus Foundation for a New Faculty Award. Support from the National Science Foundation (Grants CHE-0846402 and CHE-0840464), from the Welch Foundation (Grant A-1658), and from Texas A&M University startup funds is gratefully acknowledged. We thank

Dr. Gao for valuable discussions. We also thank Ms. Whitney Ajie for assistance in the preparation of the manuscript and J. Martin Scholtz for allowing the use of a CD spectrometer.

## ■ ABBREVIATIONS

CD: circular dichroism; NOE: nuclear Overhauser effect; ROE: rotating frame Overhauser effect; trpzip: tryptophan zipper peptide

## ■ REFERENCES

- (1) Cochran, A. G.; Skelton, N. J.; Starovasnik, M. A. *Proc. Natl. Acad. Sci. U.S.A.* **2001**, *98*, 5578.
- (2) Huang, R.; Wu, L.; McElheny, D.; Bour, P.; Roy, A.; Keiderling, T. A. *J. Phys. Chem. B* **2009**, *113*, 5661.
- (3) Du, D. G.; Zhu, Y. J.; Huang, C. Y.; Gai, F. *Proc. Natl. Acad. Sci. U.S.A.* **2004**, *101*, 15915.
- (4) Yang, W. Y.; Pitera, J. W.; Swope, W. C.; Gruebele, M. *J. Mol. Biol.* **2004**, *336*, 241.
- (5) Wu, L.; McElheny, D.; Huang, R.; Keiderling, T. A. *Biochemistry* **2009**, *48*, 10362.
- (6) Takekiyo, T.; Wu, L.; Yoshimura, Y.; Shimizu, A.; Keiderling, T. A. *Biochemistry* **2009**, *48*, 1543.
- (7) Hughes, R. M.; Waters, M. L. *Curr. Opin. Struct. Biol.* **2006**, *16*, 514.
- (8) Kiehna, S. E.; Waters, M. L. *Protein Sci.* **2003**, *12*, 2657.
- (9) Tatko, C. D.; Waters, M. L. *J. Am. Chem. Soc.* **2002**, *124*, 9372.
- (10) Zhang, J.; Qin, M.; Wang, W. *Proteins* **2006**, *62*, 672.
- (11) Yang, L.; Shao, Q.; Gao, Y. Q. *J. Phys. Chem. B* **2009**, *113*, 803.
- (12) Shao, Q.; Gao, Y. Q. *J. Chem. Theory Comput.* **2010**, *6*, 3750.
- (13) Keller, R. Ph.D. Thesis, Diss. ETH Nr. 15947, The Swiss Federal Institute of Technology, Zürich, 2004.
- (14) Glickson, J. D.; Urry, D. W.; Havran, R. T.; Walter, R. *Proc. Natl. Acad. Sci. U.S.A.* **1972**, *69*, 2136.
- (15) Llinas, M.; Klein, M. P.; Neilands, J. B. *J. Mol. Biol.* **1970**, *52*, 399.
- (16) Llinas, M.; Neilands, J. B. *Biophys. Struct. Mech.* **1976**, *2*, 105.
- (17) Baxter, N. J.; Williamson, M. P. *J. Biomol. NMR* **1997**, *9*, 359.
- (18) Mahalakshmi, R.; Raghothama, S.; Balaram, P. *J. Am. Chem. Soc.* **2006**, *128*, 1125.
- (19) Gellman, S. H.; Dado, G. P.; Liang, G. B.; Adams, B. R. *J. Am. Chem. Soc.* **1991**, *113*, 1164.
- (20) Otlewski, T. C. J. *J. Biomol. NMR* **2001**, *21*, 249.
- (21) Wishart, D. S.; Sykes, B. D.; Richards, F. M. *Biochemistry* **1992**, *31*, 1647.
- (22) Wüthrich, K. *NMR of Proteins and Nucleic Acids*; Wiley: New York, 1986.
- (23) Cavanagh, J. *Protein NMR Spectroscopy: Principles and Practice*; Academic Press: San Diego, CA, 1996.
- (24) Luginbühl, P.; Wüthrich, K. *Prog. Nucl. Magn. Reson. Spectrosc.* **2002**, *40*, 199.
- (25) Lipari, G.; Szabo, A. J. *J. Am. Chem. Soc.* **1982**, *104*, 4546.
- (26) Lide, D. R. *CRC Handbook of Chemistry and Physics*, 91st ed.; CRC Press, Inc.: Boca Raton, FL, 2010.
- (27) Kay, L. E.; Torchia, D. A.; Bax, A. *Biochemistry* **1989**, *28*, 8972.
- (28) Marlow, M. S.; Wand, A. J. *Biochemistry* **2006**, *45*, 8732.
- (29) Chugh, P.; Oas, T. G. *Biochemistry* **2007**, *46*, 1141.
- (30) Shojania, S.; O'Neil, J. D. *J. Biol. Chem.* **2006**, *281*, 8347.
- (31) Krishna, M. M.; Hoang, L.; Lin, Y.; Englander, S. W. *Methods* **2004**, *34*, 51.